Article

Body Composition Metrics Associated with Time to Progression in Smoldering Multiple Myeloma

Fabian Bauer [1,2,3,*], Florian A. Huber [1,4], Marilyn E. Galdamez [1,5,6], Ivanna Zorgno [1,5,6], Sina Habibollahi [7], Amine El Kandoussi [1], Florian J. Fintelmann [8], P. Erik Tonnesen [8,9], Anna-Sophia W. Dietrich [8,10], Zhe Wang [1], Adam Graeber [11], Robert D. Boutin [12], Leon Lenchik [13], Joshua N. Gustine [14], Steven J. Staffa [15], Noopur Raje [14] and Connie Y. Chang [1]

1 Division of Musculoskeletal Imaging and Intervention, Department of Radiology, Massachusetts General Hospital and Harvard Medical School, Boston, MA 02114, USA; cychang@mgh.harvard.edu (C.Y.C.)
2 Division of Radiology, German Cancer Research Center, 69120 Heidelberg, Germany
3 Institute for Diagnostic and Interventional Radiology, Faculty of Medicine and University Hospital Cologne, University of Cologne, 50937 Cologne, Germany
4 Institute of Diagnostic and Interventional Radiology, University Hospital Zurich, Faculty of Medicine, University of Zurich, 8091 Zurich, Switzerland
5 Metabolic Imaging Core, Nutrition Obesity Research Center at Harvard, Massachusetts General Hospital, Harvard Medical School, Boston, MA 02114, USA
6 Cardiovascular Imaging Research Center, Department of Radiology, Massachusetts General Hospital, Harvard Medical School, Boston, MA 02114, USA
7 Department of Radiology, Yale New Haven Health- Bridgeport Hospital, Bridgeport, CT 06610, USA
8 Division of Thoracic Imaging and Intervention, Department of Radiology, Massachusetts General Hospital and Harvard Medical School, Boston, MA 02114, USA
9 Department of Radiology and Nuclear Medicine, University Hospital Schleswig-Holstein, 23538 Lubeck, Germany
10 Department of Internal Medicine I, University Hospital Frankfurt, Goethe University, 60590 Frankfurt am Main, Germany
11 Department of Radiology, Brooke Army Medical Center, Fort Sam Houston, TX 78234, USA; adamgraeber@gmail.com
12 Department of Radiology, University of California Davis School of Medicine, Sacramento, CA 95817, USA
13 Department of Radiology, Wake Forest University School of Medicine, Medical Center Boulevard, Winston-Salem, NC 27157, USA
14 Center for Multiple Myeloma, Massachusetts General Hospital Cancer Center and Harvard Medical School, Boston, MA 02114, USA; nraje@mgh.harvard.edu (N.R.)
15 Department of Anesthesiology and Surgery, Boston Children's Hospital, Boston, MA 02115, USA
* Correspondence: fabian.bauer@uk-koeln.de

Abstract

Objective: To determine the association of body composition (BC) in smoldering multiple myeloma (SMM) with time to progression (TTP) to MM. **Methods**: The quantity and quality of adipose and muscle tissue were retrospectively derived from 63 whole-body low-dose computed tomography (WBLDCT) scans between 2017 and 2021. BC was analyzed by segmenting a single axial image at the level of the fourth lumbar vertebrae. Subjects were grouped into below vs. above the sex-specific median for BC metrics. Clinical information including TTP and progression risk factors were recorded. Cox proportional hazard models were used to determine the association between BC metrics and TTP. BC groups were compared using the Wilcoxon rank sum test and Fisher's exact test. **Results**: Thirty subjects progressed over a median follow-up of 49.2 months. For subjects with a subcutaneous adipose tissue (SAT) cross-sectional area (CSA) below vs. above the median, TTP was 24.8 vs. not reached ($p = 0.02$). Similarly, TTP was 20.7 vs. not reached ($p = 0.01$) for those with SAT CSA indexed to height below vs. above the median. High SAT CSA (hazard ratio [HR]: 0.42 [95%CI: 0.20–0.90], $p = 0.03$) and high SAT index (HR: 0.39 [95%CI: 0.18–0.83], $p = 0.01$) were both associated with a lower progression risk. High SAT index remained significantly

associated with reduced progression risk in multivariate analysis (p = 0.03). There was no association between TTP and obesity (BMI $\geq$ 30 kg/m^2) or muscle metrics. High SAT CSA and index were associated with younger age and higher hemoglobin levels. **Conclusions**: SAT quantity might serve as a prognostic marker for progression in SMM.

Keywords: smoldering multiple myeloma; body composition; computed tomography; time to progression

1. Introduction

Smoldering multiple myeloma (SMM) is a precursor to multiple myeloma (MM) with varying time to progression (TTP) and outcomes [1]. In SMM, median TTP is 5 years with 73% of SMM patients progressing within 15 years of diagnosis [2]. Current management strategies of precursor diseases rely on evaluating patient characteristics and myeloma-specific factors predictive of progression to MM [3–9]. The Mayo 20/2/20 risk stratification system categorizes SMM patients into distinct risk groups based on a serum-free light chain ratio (SFLCR) of more than 20, a monoclonal protein (m-protein) concentration of more than 2.0 g/dL, and plasma cell infiltration of more than 20% [7]. An updated version includes high-risk cytogenetic aberrations as an additional criterion [8]. Recently, the PANGEA models demonstrated superior predictive accuracy for progression in monoclonal gammopathy of unknown significance (MGUS) and SMM by incorporating time-varying biomarkers such as SFLCR, m-protein, serum creatinine, hemoglobin, age, and optionally plasma cell infiltration [3].

To rule out myeloma-defining lytic lesions [10], the International Myeloma Working Group (IMWG) recommends whole-body low-dose CT (WBLDCT) as the first-line imaging modality for suspected (S)MM and high-risk MGUS [11]. Beyond providing the diagnosis of myeloma, WBLDCT also offers opportunistic insights into body composition (BC). BC is typically assessed using a single cross-sectional CT image at the L3 or L4 lumbar level to estimate skeletal muscle and adipose tissue quality and quantity [12]. Sarcopenia, characterized by low muscle mass, function, or quality, has been previously established as a significant predictor of morbidity and mortality across various cancer entities [13–18]. In MM, various studies have evaluated the association between sarcopenia and disease features or outcomes, reporting discordant results [19–27]. Similarly, BC metrics capturing the distribution and quality of abdominal adipose tissue were investigated for their impact on outcome, again with diverging results [19,20,24,26,28]. While BC analysis has been extensively studied in MM, there is limited information on the value of BC in SMM.

This study aimed to investigate the prognostic value of BC metrics opportunistically derived from baseline WBLDCT in subjects with SMM. We hypothesized that BC metrics assessing muscle mass and adipose tissue in both quality and quantity could serve as additional imaging biomarkers for progression.

2. Materials and Methods

This retrospective cohort study received approval from the Institutional Review Board (Control Number 2021P001575) with a waiver of individual informed consent and was compliant with the Health Insurance Portability and Accountability Act (HIPAA).

2.1. Study Cohort and Data Collection

The Picture Archiving and Communication System of a tertiary care academic hospital was searched for consecutive WBLDCT scans performed between July 2017 and March

2021. Inclusion required a diagnosis of SMM at the time of WBLDCT, a follow-up period of more than 3 months, and no diagnosis of MM within three months following the WBLDCT. Incomplete imaging and prior myeloma treatment led to exclusion. Clinical data were collected from the electronic health record. Clinical information collected within 90 days of the WBLDCT exam included patient characteristics (age, sex, body mass index [BMI]), smoking status, and a diagnosis of diabetes mellitus type II. Positive smoking status was defined as ≥5 pack-years. Laboratory parameters included serum creatine, hemoglobin, m-protein, plasma cell infiltration, and SFLCR.

The primary outcome of interest was TTP, defined as the time from when the WBLDCT was performed until disease progression to MM. Subjects without an event at the end of follow-up were censored. Outcome data were retrieved in May 2024. Diagnosis of SMM and MM was made using the IMWG criteria [10].

2.2. Image Analysis

Non-contrast helical WBLDCT scans were performed using helical CT scanners from multiple manufacturers, including Siemens Healthcare (Erlangen, Germany), GE Healthcare (Milwaukee, WI, USA), Canon Medical Systems Corporation (Ōtawara, Japan), and Philips Professional Healthcare (Amsterdam, The Netherlands). The acquisition parameters were as follows: section thickness of 1.5–3.0 mm, pitch between 1.0 and 1.2, rotation time of 0.4–0.5 s, field of view of 50 cm, tube voltage of 120 kVp, tube current between 16 and 199 mAs, a mean CT dose index volume of 4.5 ± 1.4 mGy, and a mean dose-length product of 628.1 ± 181.8 mGy·cm.

Regions of interest of the different tissues were determined at the midpoint of the L4 vertebral body using previously validated segmentation models [8]. A standard single slice was manually determined by one of the authors (MEG) with four years of experience in medical imaging and trained by senior fellowship-trained musculoskeletal radiologists (Figure 1). All segmentations were manually inspected and corrected, if necessary, by two of the authors (MEG and IZ) using Horos DICOM viewer version 3.3.6 (www.horosproject.com (accessed on 05/15/2024)). BC analysis was conducted blinded to clinical information and outcomes.
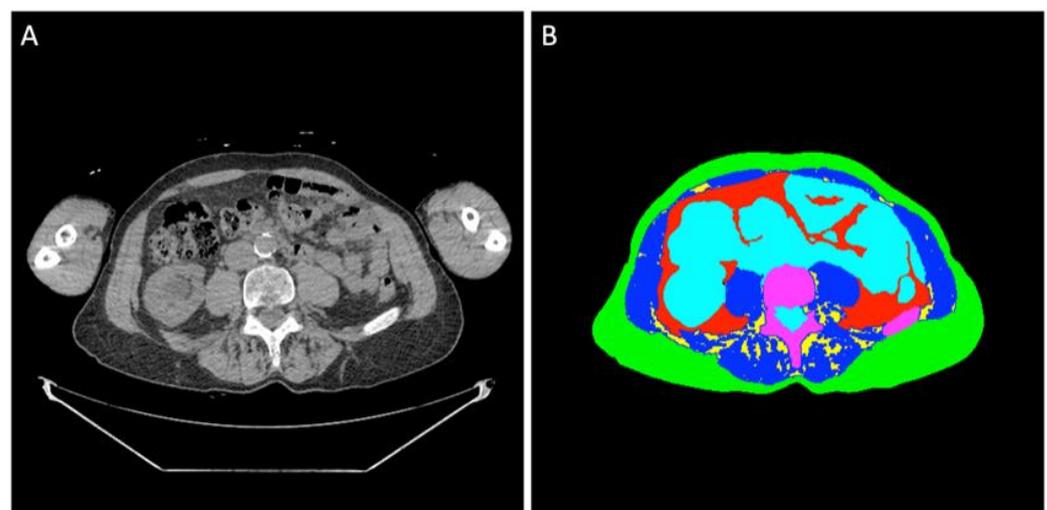
Figure 1. (**A**) Non-contrast WBLDCT image at L4 level of an 80-year-old man diagnosed with SMM. (**B**) Semi-automated segmentation of the abdominal tissue: green label: subcutaneous adipose tissue; red label: visceral adipose tissue; yellow label: intermuscular adipose tissue; blue label: muscle tissue; turquoise label: organs, vessels, fluids; purple label: bone.

BC analysis included the mean radiodensity in Hounsfield Units (HU) and cross-sectional area (CSA) of the abdominal subcutaneous adipose tissue (SAT), visceral adipose tissue (VAT), intermuscular adipose tissue (IMAT), and the skeletal muscle. The SAT index, VAT index, IMAT index, TAT index, and skeletal muscle index were calculated by dividing the respective CSAs by patient height in meters squared. Total adipose tissue (TAT) was calculated as the sum of the SAT, VAT, and IMAT. Skeletal muscle included all paraspinal, abdominal, paraspinal, and psoas muscle.

2.3. Statistical Analysis

Categorical variables were summarized as proportions. Continuous variables were summarized as medians with their respective interquartile ranges (IQR). The study cohort was divided into groups based on the sex-specific median for the respective BC metrics. Myopenia and myosteatosis were defined using the following independently established sex-specific cutoffs from the literature. For myopenia (skeletal muscle index), cutoffs were <55 cm^2/m^2 in men and <39 cm^2/m^2 in women for skeletal muscle index [29]. For myosteatosis (skeletal muscle radiodensity), cutoffs were <28.1 HU in men and <18.9 HU in women [30].

TTP with 95% confidence intervals (95%CI) was calculated using the Kaplan–Meier method. TTP of the resulting groups was compared using the log-rank test. Univariate Cox regression analysis was conducted to evaluate the association of progression risk with individual BC metrics. The results of the Cox regression analyses were presented as hazard ratios (HR) with 95% CI. BC metrics significant in univariate analysis were analyzed using multivariable regression. Multivariable analysis was performed by adding prior selected known risk factors for progression to MM as defined in the PANGEA models, adjusting for SFLCR, m-protein, serum creatinine, hemoglobulin, and age [3]. Due to data availability, the plasma cell infiltration was not included in the multivariable analysis. Groups based on the respective BC cutoff were compared for the continuous clinical parameters using the Wilcoxon rank sum test and for nominal parameters using Fisher's exact test.

A two-sided *p*-value of <0.05 was considered statistically significant. Statistical analysis was performed using Python 3.9 with pandas, lifelines, numpy, and matplotlib packages, and using Stata 18.1 (StataCorp LLC, College Station, TX, USA).

3. Results

3.1. Baseline Characteristics

A total of 63 WBLDCT scans from 63 subjects met eligibility criteria for BC analysis (Figure 2). The median age of the cohort was 69 years, with 41% of the study subjects being male. The median BMI was 27 kg/m^2, and 19% of subjects had a diagnosis of diabetes mellitus. Of the entire cohort, 2% were classified as underweight (BMI < 18.5 kg/m^2), 24% had normal weight (BMI 18.5 to <25 kg/m^2), 46% were overweight (BMI 25 to <30 kg/m^2), and 28% were obese (BMI ≥ 30 kg/m^2). Further details of the baseline characteristics are provided in Table 1.

After a median follow-up of 49.2 months (95%CI: 41.6–53.7), 30 study subjects with 30 WBLDCT scans (48%) progressed to MM. The median TTP was 41.9 months (95%CI: 23.2-not reached [NR]). There was no significant difference between patients who progressed and those who did not in baseline characteristics ($p \geq 0.11$).
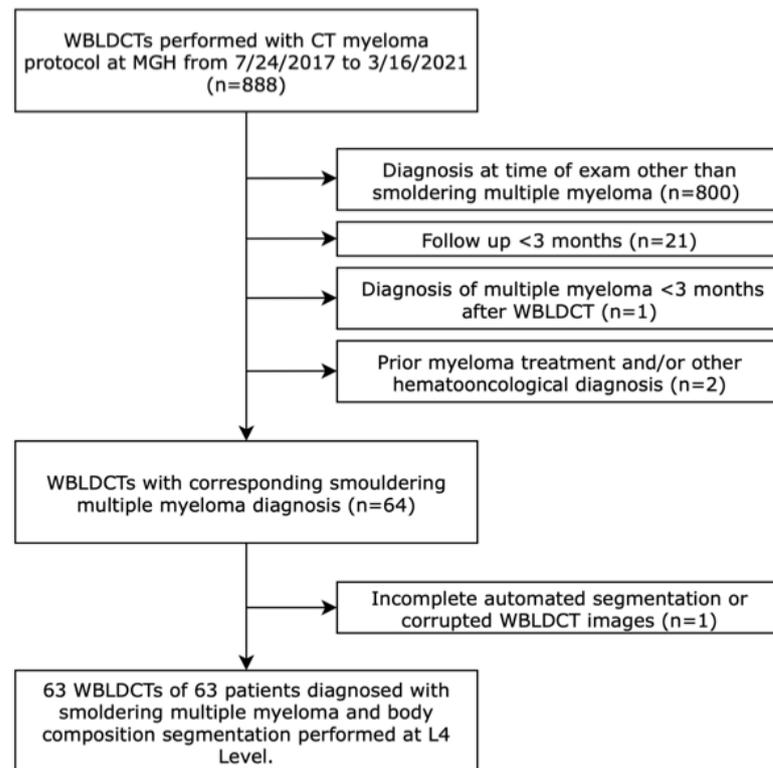
Figure 2. Flowchart. WBLDCT: whole-body low-dose CT.

Table 1. Baseline patient characteristics.

	Total	**Not Progressed**	**Progressed**	*p*-**Value**
WBLDCT	63	33	30	
Subjects	63	33	30	
Male sex	26 (41)	11 (33)	15 (50)	0.21
Age in years	69 (64–75)	68 (63–75)	71 (66–75)	0.42
BMI in kg/m^2	27 (25–30)	28 (25–31)	27 (25–29)	0.44
Diabetes mellitus type II	12 (19)	9 (27)	3 (10)	0.11
Smoking $\geq$ 5 pack-years	24 (38)	12 (36)	12 (40)	0.80
SFLCR	13 (4–63)	9 (3–18)	27 (8–79)	0.44
Serum creatinine in mg/dL	0.9 (0.8–1.1)	0.9 (0.8–1.1)	0.9 (0.8–1.2)	0.46
Hemoglobin in g/dL	12.6 (11.7–13.6)	12.7 (11.8–13.6)	12.6 (11.7–13.6)	0.60
M-protein in g/L [n missing values]	1.3 (0.6–1.9) [13]	0.8 (0.3–1.4) [20]	1.6 (1.1–2.2) [20]	0.33
PCI in % [n missing values]	15 (10–20) [31]	15 (8–20) [5]	18 (10–20) [32]	0.26

Data is presented as median (interquartile range) for continuous variables and n (%) for categorical variables. Abbreviations: BMI: body mass index; SFLCR: serum-free light chain ratio; m-protein: monoclonal protein; PCI: plasma cell infiltration; WBLDCT: whole-body low-dose CT.

3.2. Impact of Adipose Tissue

Sex-specific median values for adipose tissue BC metrics are presented in Table 2. TTP was 24.8 months vs. NR for subjects with SAT CSA below vs. above the median, respectively (*p* = 0.02). When indexed to height, TTP was 20.7 months for subjects below the median and NR for those above the median (*p* = 0.01, Figure 3). No significant differences in TTP were observed for groups divided into below vs. above the respective median on SAT radiodensity or BC metrics based on VAT, TAT, or IMAT (Table 2).

Table 2. Association between body composition analysis metrics and time to progression in smoldering multiple myeloma.

Body Composition Metric	Median Males (IQR)	Median Females (IQR)	TTP Based on Median in Months (95%CI): Below vs. Above
Adipose Tissue			
SAT CSA in cm^2	213.2 (187.5, 271.1)	273.1 (185.6, 336.2)	24.8 (13.8–41.9) vs. NR (32.1-NR), $p = 0.02$
SAT Index in cm^2/m^2	74.4 (63.7, 93.7)	101.6 (72.9, 125.0)	20.7 (13.2–36.1) vs. NR (41.9-NR), $p = 0.01$
SAT Radiodensity in HU	−89.0 (−95.7, −79.1)	−100.5 (−104.0, −93.4)	36.1 (19.1-NR) vs. NR (18.4-NR), $p = 0.47$
VAT CSA in cm^2	170.5 (114.4, 222.4)	128.8 (55.7, 177.0)	36.1 (19.6-NR) vs. NR (12.7-NR), $p = 0.61$
VAT Index in cm^2/m^2	59.3 (36.3, 76.2)	45.8 (20.4, 71.7)	36.1 (19.6-NR) vs. NR (12.7-NR), $p = 0.61$
VAT Radiodensity in HU	−96.2 (−101.6, −93.6)	−96.5 (102.0, −87.9)	36.1 (11.3-NR) vs. NR (19.6-NR), $p = 0.38$
IMAT CSA in cm^2	3.2 (1.7, 7.1)	3.0 (1.6, 7.0)	47.2 (24.8-NR) vs. NR (12.7-NR), $p = 0.73$
IMAT Index in cm^2/m^2	1.3 (0.5, 2.5)	1.0 (0.7, 2.6)	47.2 (24.8-NR) vs. NR (12.7-NR), $p = 0.76$
TAT CSA in cm^2	399.6 (337.7, 518.5)	435.9 (258.6, 494.9)	29.7 (18.4-NR) vs. NR (23.2-NR), $p = 0.18$
TAT Index in cm^2/m^2	133.6 (108.7, 162.2)	161.9 (101.2, 193.6)	30.3 (19.1-NR) vs. NR (13.2-NR), $p = 0.42$
Muscle Tissue			
Skeletal Muscle Index [a] in cm^2/m^2	59.8 (53.6, 66.5)	48.5 (43.6, 53.8)	18.4 (5.8–41.9) vs. NR (29.7-NR), $p = 0.07$
Skeletal Muscle Radiodensity [b] in HU	22.5 (18.2, 30.8)	16.2 (7.8, 20.9)	41.9 (13.2-NR) vs. 47.2 (19.6-NR), $p = 0.59$

[a] Reference cutoff used for myopenia: skeletal muscle index < 55.0 cm^2/m^2 for males and <39.0 cm^2/m^2 for females. [b] Reference cutoff used for myosteatosis: skeletal muscle radiodensity < 28.1 HU in males and <18.9 HU in females. Abbreviations: CI: confidence interval; CSA: cross-sectional area; HU: Hounsfield Unit; IMAT: intermuscular adipose tissue; IQR: interquartile range; NR: not reached; SAT: subcutaneous adipose tissue; TAT: total adipose tissue; TTP: time to progression; VAT: visceral adipose tissue;

In univariate analysis, high SAT CSA (HR: 0.42 [95%CI: 0.20–0.90], $p = 0.03$) and index (HR: 0.39 [95%CI: 0.18–0.83], $p = 0.01$) were associated with a lower risk of progression to MM. In multivariable analysis, adjusting for age, serum creatinine, hemoglobin, SFLC-ratio, and m-protein, high SAT index was independently associated with a lower progression risk (HR: 0.37 [95%CI: 0.15–0.90], $p = 0.03$). There were no significant associations with progression for SAT radiodensity or BC metrics based on VAT, TAT, or IMAT above vs. below the median cutoff.

Subjects with SAT CSA above the median were younger (68.0 vs. 73.0 years, $p = 0.05$) and had higher hemoglobin levels (13.2 vs. 12.0 g/dL, $p = 0.01$). Similarly, high SAT index was associated with younger age (68.0 vs. 72.0 years, $p = 0.03$) and higher hemoglobin level (13.2 vs. 12.0 g/dL, $p = 0.01$) (Table 3). Both high SAT CSA and SAT index were associated with obesity, with 42% of subjects above the median for those BC metrics classified as obese compared to 16% below the median ($p = 0.03$).
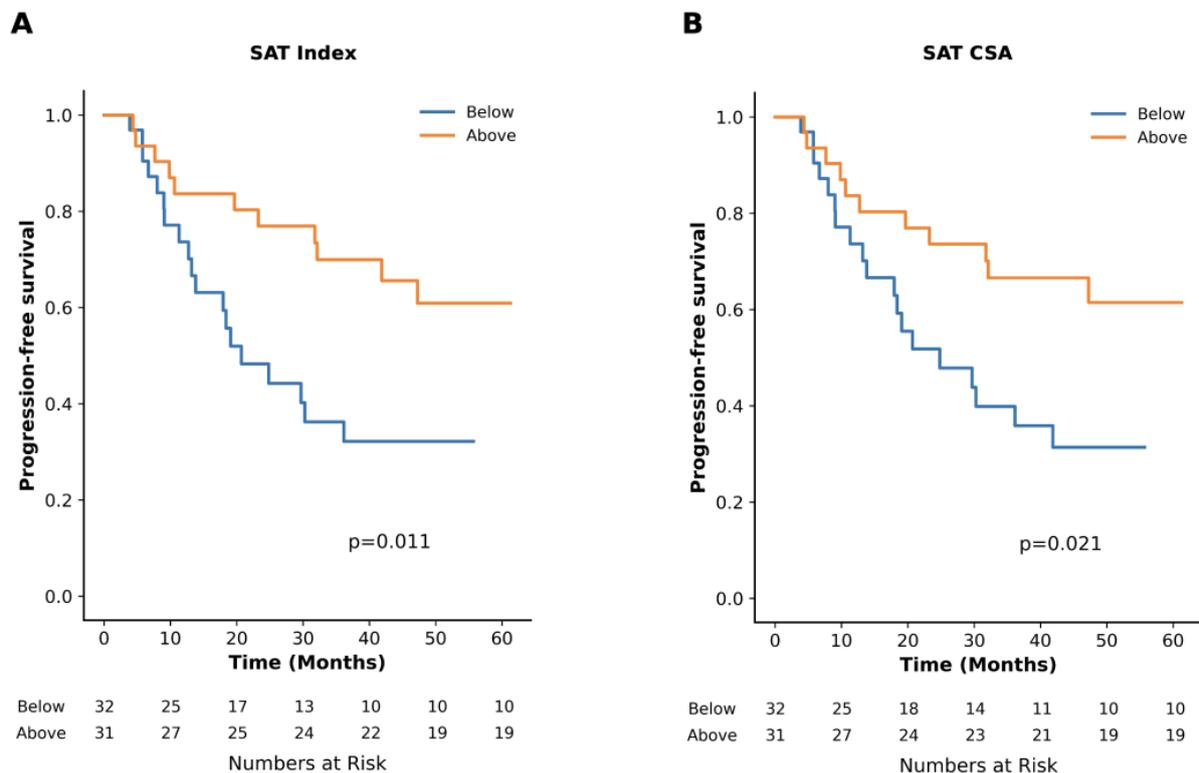
Figure 3. Time to progression (TTP) and subcutaneous adipose tissue cross-sectional area (SAT CSA) and index. (**A**) TTP (months) of subjects with SAT index above the sex-specific median compared to those below. (**B**) TTP (months) of subjects with SAT CSA above the sex-specific median compared to those below.

Table 3. Association between subcutaneous adipose tissue index and subcutaneous adipose tissue cross-sectional area and risk factors for progression.

	SAT Index			SAT CSA		
	Below	**Above**	*p*-Value	**Below**	**Above**	*p*-Value
Age in years	73.0	68.0	0.03	72.0	68.0	0.05
Serum creatinine in mg/dL	0.9	0.9	0.84	0.91	9.0	0.91
Hemoglobin in g/dL	12.0	13.2	<0.01	12.0	13.2	0.01
SFLCR	13.9	11.4	0.14	13.1	12.5	0.24
M-protein in g/L	1.3	1.4	0.57	13.3	14.0	0.83

Risk factors (median) are given for groups above vs. below the sex-specific median of the respective body composition metric. Abbreviations: CSA: cross-sectional area; m-protein: monoclonal protein; SAT: subcutaneous adipose tissue; SFLCR: serum-free light chain ratio.

3.3. Impact of Skeletal Muscle

Sex-specific median values for the BC metrics for muscle tissue are provided in Table 2. According to predefined sex-specific cutoffs for myopenia [29] and myosteatosis [30], the prevalence of myopenia was 31% in men and 11% in women, while myosteatosis was observed in 65% of men and 62% of women. Of the patients that progressed to MM, 27% had myopenia and 63% had myosteatosis, whereas 12% and 64% of the patients without progression to MM had myopenia and myosteatosis, respectively.

There was a trend for shorter TTP in patients with myopenia (18.4 months vs. NR, *p* = 0.07). TTP was 41.9 months for subjects with myosteatosis and 47.2 months for those

without ($p = 0.59$). Myopenia was not associated with age, serum creatinine, hemoglobin, SFLCR, or m-protein ($p \geq 0.12$). Among subjects with and without myopenia, 9% and 50% were classified as obese, respectively ($p = 0.15$). Myosteatosis was associated with older age (72.5 vs. 65.0 years, $p = 0.01$). No associations were found between myosteatosis and serum creatinine, hemoglobin, SFLCR, and m-protein ($p \geq 0.32$). Additionally, 48% of subjects with myosteatosis were obese, compared to 28% of those without ($p = 0.40$).

4. Discussion

In this study, we demonstrated that BC metrics derived from WBLDCT using semi-automated image analysis pipelines are independently associated with TTP from SMM to MM. Our study shows that quantitatively assessed high SAT was independently associated with lower risk of progression and longer TTP and was linked to risk factors for progression.

Several studies have investigated the prognostic value of quantifying the abdominal adipose tissue in myeloma spectrum disease. Abdallah et al. reported that in 341 patients with MM, those in the lower and higher tertiles for SAT CSA had decreased overall survival compared to the middle tertile. However, TAT or VAT CSA were not associated with the outcome [19]. In a study cohort of 56 patients newly diagnosed with MM, a SAT index below the median predicted poor survival [26]. In a case-control study, Veld et al. reported that patients with MM exhibited increased TAT and SAT CSA as well as higher VAT metabolic activity in FDG-PET/CT compared to those diagnosed with MGUS [33]. In a population-based study including 300 patients with MGUS, no association between BC metrics and MGUS prevalence or progression to SMM after a median follow-up of 8 years was found [34]. Notably, discordant results in prior studies can be partially explained by variability in the study populations and different thresholds used to define BC metrics. In our study, SAT CSA and index were independently (SAT index) associated with decreased risk of progression after adjusting for risk factors for progression defined in the PANGEA models [3]. Additionally, high SAT CSA and index were associated with lower age and higher hemoglobin. These findings suggest that SAT CSA or index could serve as imaging biomarkers for assessing the risk of progression to MM in SMM. With WBLDCT routinely performed in the diagnostic algorithm for (S)MM [11,35,36], the assessment of SAT quantity could be performed opportunistically, offering potential support in clinical decision making.

VAT is more metabolically active than SAT and has a pro-inflammatory adipokine profile [37], which could potentially promote carcinogenesis [38]. For example, low levels of adiponectin, an anti-inflammatory adipokine inversely associated particularly with visceral obesity [39,40], have been linked to a higher risk of MM [41]. While increased VAT CSA was associated with adverse cytogenetics and treatment response in MM [42], our findings suggest that SAT may play a distinct, possibly protective role in SMM. It is also possible that in SMM, lower SAT could potentially be a result of increased tumor activity, where increased lipolysis and subsequent depletion of SAT could occur as the tumor progresses, ultimately leading to the diagnosis of active MM. Recent studies have highlighted that cancer-associated adipocytes in the bone marrow interact with tumor cells in a variety of metabolic mechanisms [43]. Further studies are needed to clarify the precise role of BC metrics and adipocytes and their metabolic pathways in MM progression.

The role of BMI in myeloma spectrum disease has been inconsistently reported, with some studies linking higher BMI to higher progression risk and incidence of MM [44] and MGUS [45–47], while others found no or limited association [31,34,48]. Additionally, in MM, being underweight [49,50] and severe obesity [50] were associated with poor survival. In our cohort, BMI and obesity were not associated with time to progression, suggesting that quantitative body composition metrics may provide a more sensitive assessment than BMI alone.

Although myopenia and myosteatosis with varying cutoffs have been associated with adverse outcomes in MM [21–23,25,27], results across studies are inconsistent [19,20,24,26]. In our cohort of SMM patients, neither parameter correlated with progression, suggesting that muscle alterations may become more clinically relevant in later disease stages.

Recent evidence highlights the prognostic value of advanced imaging modalities such as PET-CT and whole-body MRI in SMM, particularly for assessing focal marrow disease and early progression [32,51,52]. Importantly, body composition analysis is not limited to CT; quantitative metrics can also be derived from MRI or PET-CT, offering a complementary perspective. Incorporating BC assessment into multimodal imaging protocols may therefore enable a more comprehensive characterization of disease biology and progression risk.

This exploratory study has several limitations, including its retrospective design with potential selection bias and limited sample size. The exclusion of cytogenetic aberrations and plasma cell infiltration due to incomplete data may have influenced our multivariable analysis outcomes. Given the limited sample size, we refrained from testing alternative skeletal muscle cutoffs to avoid data-driven bias and maintain comparability with prior studies. Notably, different cutoff definitions have been shown to result in variable clinical impact on survival outcomes [53]. Additionally, our study relied on a single time point for BC analysis, which may not capture the dynamic changes in BC during disease progression. As our institution is a tertiary referral center, the exact timing of CT acquisition relative to SMM diagnosis was not available for all patients, which may have introduced bias in the time to progression analysis. Larger prospective future studies with a separate validation cohort are needed to validate our findings.

Our study demonstrated that BC analysis in WBLDCT provides prognostic information in patients with SMM. High SAT quantity was independently associated with a lower risk of progression and might serve as a predictive imaging biomarker for progression to MM in SMM. Analyzing adipose tissue composition through CT, rather than relying solely on BMI or total adipose tissue, could provide additional insights into assessing individual progression risks in SMM.

Institutional Review Board Statement: All procedures performed in studies involving human subjects were in accordance with the ethical standards of the institutional and/or national research committee and with the 1964 Helsinki declaration and its later amendments or comparable ethical standards. This study was approved by the Mass General Brigham (MGB) Human Research IRB (Protocol #: 2021P001575, approval date 1 April 2021).

Informed Consent Statement: The study was approved by the local Institutional Review Board (IRB) and HIPAA compliant. Verbal consent for participation in the study was waived due to retrospective study design.

Data Availability Statement: The datasets generated during and/or analyzed during the current study are available from the corresponding author upon reasonable request.

Conflicts of Interest: F.J.F. reports research funding from Pfizer, consulting for B.D. and Boston Scientific, and holds a patent related to body composition analysis. The other authors declare that they have no conflicts of interest.

Abbreviations

BC: body composition; BMI: body-mass index; CI: confidence interval; CSA: cross-sectional area; HU: Hounsfield Unit; IMAT: intermuscular adipose tissue; MM: multiple myeloma; m-protein: monoclonal protein; NR: not reached; SAT: subcutaneous adipose tissue; SFLCR: serum-free light chain ratio; SMM: smoldering multiple myeloma; TAT: total adipose tissue; TTP: time to progression; VAT: visceral adipose tissue; WBLDCT: whole-body low-dose CT.

References

1. Kumar, S.K.; Rajkumar, V.; Kyle, R.A.; van Duin, M.; Sonneveld, P.; Mateos, M.V.; Gay, F.; Anderson, K.C. Multiple myeloma. *Nat. Rev. Dis. Primers* **2017**, *3*, 17046. [CrossRef]
2. Kyle, R.A.; Remstein, E.D.; Therneau, T.M.; Dispenzieri, A.; Kurtin, P.J.; Hodnefield, J.M.; Larson, D.R.; Plevak, M.F.; Jelinek, D.F.; Fonseca, R.; et al. Clinical course and prognosis of smoldering (asymptomatic) multiple myeloma. *N. Engl. J. Med.* **2007**, *356*, 2582–2590. [CrossRef]
3. Cowan, A.; Ferrari, F.; Freeman, S.S.; Redd, R.; El-Khoury, H.; Perry, J.; Patel, V.; Kaur, P.; Barr, H.; Lee, D.J.; et al. Personalised progression prediction in patients with monoclonal gammopathy of undetermined significance or smouldering multiple myeloma (PANGEA): A retrospective, multicohort study. *Lancet Haematol.* **2023**, *10*, e203–e212. [CrossRef] [PubMed]
4. Hughes, D.; Yong, K.; Ramasamy, K.; Stern, S.; Boyle, E.; Ashcroft, J.; Basheer, F.; Rabin, N.; Pratt, G. Diagnosis and management of smouldering myeloma: A British Society for Haematology Good Practice Paper. *Br. J. Haematol.* **2024**, *204*, 1193–1206. [CrossRef]
5. Kunacheewa, C.; Manasanch, E.E. High-risk smoldering myeloma versus early detection of multiple myeloma: Current models, goals of therapy, and clinical implications. *Best Pract. Res. Clin. Haematol.* **2020**, *33*, 101152. [CrossRef]
6. Kyle, R.A.; Durie, B.G.; Rajkumar, S.V.; Landgren, O.; Blade, J.; Merlini, G.; Kroger, N.; Einsele, H.; Vesole, D.H.; Dimopoulos, M.; et al. Monoclonal gammopathy of undetermined significance (MGUS) and smoldering (asymptomatic) multiple myeloma: IMWG consensus perspectives risk factors for progression and guidelines for monitoring and management. *Leukemia* **2010**, *24*, 1121–1127. [CrossRef]
7. Lakshman, A.; Rajkumar, S.V.; Buadi, F.K.; Binder, M.; Gertz, M.A.; Lacy, M.Q.; Dispenzieri, A.; Dingli, D.; Fonder, A.L.; Hayman, S.R.; et al. Risk stratification of smoldering multiple myeloma incorporating revised IMWG diagnostic criteria. *Blood Cancer J.* **2018**, *8*, 59. [CrossRef] [PubMed]
8. Mateos, M.V.; Kumar, S.; Dimopoulos, M.A.; Gonzalez-Calle, V.; Kastritis, E.; Hajek, R.; De Larrea, C.F.; Morgan, G.J.; Merlini, G.; Goldschmidt, H.; et al. International Myeloma Working Group risk stratification model for smoldering multiple myeloma (SMM). *Blood Cancer J.* **2020**, *10*, 102. [CrossRef]
9. van de Donk, N.W.; Mutis, T.; Poddighe, P.J.; Lokhorst, H.M.; Zweegman, S. Diagnosis, risk stratification and management of monoclonal gammopathy of undetermined significance and smoldering multiple myeloma. *Int. J. Lab. Hematol.* **2016**, *38* (Suppl. S1), 110–122. [CrossRef]
10. Rajkumar, S.V.; Dimopoulos, M.A.; Palumbo, A.; Blade, J.; Merlini, G.; Mateos, M.V.; Kumar, S.; Hillengass, J.; Kastritis, E.; Richardson, P.; et al. International Myeloma Working Group updated criteria for the diagnosis of multiple myeloma. *Lancet Oncol.* **2014**, *15*, e538–e548. [CrossRef]

11. Hillengass, J.; Usmani, S.; Rajkumar, S.V.; Durie, B.G.M.; Mateos, M.V.; Lonial, S.; Joao, C.; Anderson, K.C.; Garcia-Sanz, R.; Riva, E.; et al. International myeloma working group consensus recommendations on imaging in monoclonal plasma cell disorders. *Lancet Oncol.* **2019**, *20*, e302–e312. [CrossRef]

12. Shah, U.A.; Ballinger, T.J.; Bhandari, R.; Dieli-Cornwright, C.M.; Guertin, K.A.; Hibler, E.A.; Kalam, F.; Lohmann, A.E.; Ippolito, J.E. Imaging modalities for measuring body composition in patients with cancer: Opportunities and challenges. *J. Natl. Cancer Inst. Monogr.* **2023**, *2023*, 56–67. [CrossRef]

13. Boutin, R.D.; Lenchik, L. Value-Added Opportunistic CT: Insights Into Osteoporosis and Sarcopenia. *AJR Am. J. Roentgenol.* **2020**, *215*, 582–594. [CrossRef]

14. Boutin, R.D.; Yao, L.; Canter, R.J.; Lenchik, L. Sarcopenia: Current Concepts and Imaging Implications. *AJR Am. J. Roentgenol.* **2015**, *205*, W255–W266. [CrossRef]

15. Hanna, P.E.; Ouyang, T.; Tahir, I.; Katz-Agranov, N.; Wang, Q.; Mantz, L.; Strohbehn, I.; Moreno, D.; Harden, D.; Dinulos, J.E.; et al. Sarcopenia, adiposity and large discordance between cystatin C and creatinine-based estimated glomerular filtration rate in patients with cancer. *J. Cachexia Sarcopenia Muscle* **2024**, *15*, 1187–1198. [CrossRef] [PubMed]

16. Nipp, R.D.; Fuchs, G.; El-Jawahri, A.; Mario, J.; Troschel, F.M.; Greer, J.A.; Gallagher, E.R.; Jackson, V.A.; Kambadakone, A.; Hong, T.S.; et al. Sarcopenia Is Associated with Quality of Life and Depression in Patients with Advanced Cancer. *Oncologist* **2018**, *23*, 97–104. [CrossRef]

17. Rier, H.N.; Jager, A.; Sleijfer, S.; Maier, A.B.; Levin, M.D. The Prevalence and Prognostic Value of Low Muscle Mass in Cancer Patients: A Review of the Literature. *Oncologist* **2016**, *21*, 1396–1409. [CrossRef]

18. van Seventer, E.; Marquardt, J.P.; Troschel, A.S.; Best, T.D.; Horick, N.; Azoba, C.; Newcomb, R.; Roeland, E.J.; Rosenthal, M.; Bridge, C.P.; et al. Associations of Skeletal Muscle With Symptom Burden and Clinical Outcomes in Hospitalized Patients With Advanced Cancer. *J. Natl. Compr. Cancer Netw.* **2021**, *19*, 319–327. [CrossRef]

19. Abdallah, N.H.; Nagayama, H.; Takahashi, N.; Gonsalves, W.; Fonder, A.; Dispenzieri, A.; Dingli, D.; Buadi, F.K.; Lacy, M.Q.; Hobbs, M.; et al. Muscle and fat composition in patients with newly diagnosed multiple myeloma. *Blood Cancer J.* **2023**, *13*, 185. [CrossRef] [PubMed]

20. Barajas Ordonez, F.; Wolleschak, D.; Zeller, Y.; Hinnerichs, M.; Rodriguez-Feria, P.; Aghayev, A.; Mikusko, M.; Borggrefe, J.; Mougiakakos, D.; Surov, A. Parameters of body composition do not predict survival in patients with multiple myeloma undergoing autologous stem cell transplantation. *Leuk. Lymphoma* **2024**, *65*, 825–832. [CrossRef]

21. Diallo, T.D.; Blessing, A.I.L.; Ihorst, G.; Moller, M.D.; Jungmann, P.M.; Bamberg, F.; Herget, G.; Wasch, R.; Engelhardt, M.; Neubauer, J. Myosteatosis in multiple myeloma: A key determinant of survival beyond sarcopenia. *Skelet. Radiol.* **2024**, *54*, 275–285. [CrossRef]

22. Nandakumar, B.; Baffour, F.; Abdallah, N.H.; Kumar, S.K.; Dispenzieri, A.; Buadi, F.K.; Dingli, D.; Lacy, M.Q.; Hayman, S.R.; Kapoor, P.; et al. Sarcopenia identified by computed tomography imaging using a deep learning-based segmentation approach impacts survival in patients with newly diagnosed multiple myeloma. *Cancer* **2023**, *129*, 385–392. [CrossRef]

23. Park, S.S.; Kwag, D.; Lee, J.Y.; Jeon, Y.W.; Yahng, S.A.; Shin, S.H.; Youn, S.Y.; Min, C.K. Prognostic value of low muscle mass at the 12(th) thoracic vertebral level in multiple myeloma treated with transplantation: CAREMM-2101 study. *Diagn. Interv. Radiol.* **2023**, *29*, 596–608. [CrossRef] [PubMed]

24. Surov, A.; Benkert, F.; Ponisch, W.; Meyer, H.J. CT-defined body composition as a prognostic factor in multiple myeloma. *Hematology* **2023**, *28*, 2191075. [CrossRef]

25. Tagliafico, A.S.; Rossi, F.; Bignotti, B.; Torri, L.; Bonsignore, A.; Belgioia, L.; Domineitto, A. CT-derived relationship between low relative muscle mass and bone damage in patients with multiple myeloma undergoing stem cells transplantation. *Br. J. Radiol.* **2022**, *95*, 20210923. [CrossRef]

26. Takeoka, Y.; Sakatoku, K.; Miura, A.; Yamamura, R.; Araki, T.; Seura, H.; Okamura, T.; Koh, H.; Nakamae, H.; Hino, M.; et al. Prognostic Effect of Low Subcutaneous Adipose Tissue on Survival Outcome in Patients With Multiple Myeloma. *Clin. Lymphoma Myeloma Leuk.* **2016**, *16*, 434–441. [CrossRef] [PubMed]

27. Williams, A.; Baruah, D.; Patel, J.; Szabo, A.; Chhabra, S.; Dhakal, B.; Hari, P.; Janz, S.; Stolley, M.; D'Souza, A. Prevalence and significance of sarcopenia in multiple myeloma patients undergoing autologous hematopoietic cell transplantation. *Bone Marrow Transpl.* **2021**, *56*, 225–231. [CrossRef] [PubMed]

28. da Cunha, A.D.J.; Silveira, M.N.; Takahashi, M.E.S.; de Souza, E.M.; Mosci, C.; Ramos, C.D.; Brambilla, S.R.; Pericole, F.V.; Prado, C.M.; Mendes, M.C.S.; et al. Adipose tissue radiodensity: A new prognostic biomarker in people with multiple myeloma. *Nutrition* **2021**, *86*, 111141. [CrossRef] [PubMed]

29. Fearon, K.; Strasser, F.; Anker, S.D.; Bosaeus, I.; Bruera, E.; Fainsinger, R.L.; Jatoi, A.; Loprinzi, C.; MacDonald, N.; Mantovani, G.; et al. Definition and classification of cancer cachexia: An international consensus. *Lancet Oncol.* **2011**, *12*, 489–495. [CrossRef]

30. Nachit, M.; Horsmans, Y.; Summers, R.M.; Leclercq, I.A.; Pickhardt, P.J. AI-based CT Body Composition Identifies Myosteatosis as Key Mortality Predictor in Asymptomatic Adults. *Radiology* **2023**, *307*, e222008. [CrossRef]

31. Schmidt, B.; Debold, E.; Frank, M.; Arendt, M.; Dragano, N.; Dürig, J.; Dührsen, U.; Moebus, S.; Erbel, R.; Jöckel, K.-H.; et al. Socioeconomic Position is Positively Associated with Monoclonal Gammopathy of Undetermined Significance in a Population-based Cohort Study. *Ann. Hematol.* **2019**, *98*, 2761–2767. [CrossRef] [PubMed]

32. Hillengass, J.; Fechtner, K.; Weber, M.A.; Bauerle, T.; Ayyaz, S.; Heiss, C.; Hielscher, T.; Moehler, T.M.; Egerer, G.; Neben, K.; et al. Prognostic significance of focal lesions in whole-body magnetic resonance imaging in patients with asymptomatic multiple myeloma. *J. Clin. Oncol.* **2010**, *28*, 1606–1610. [CrossRef] [PubMed]

33. Veld, J.; O'Donnell, E.K.; Reagan, M.R.; Yee, A.J.; Torriani, M.; Rosen, C.J.; Bredella, M.A. Abdominal adipose tissue in MGUS and multiple myeloma. *Skelet. Radiol.* **2016**, *45*, 1277–1283. [CrossRef]

34. Thordardottir, M.; Lindqvist, E.K.; Lund, S.H.; Costello, R.; Burton, D.; Korde, N.; Mailankody, S.; Eiriksdottir, G.; Launer, L.J.; Gudnason, V.; et al. Obesity and risk of monoclonal gammopathy of undetermined significance and progression to multiple myeloma: A population-based study. *Blood Adv.* **2017**, *1*, 2186–2192. [CrossRef] [PubMed]

35. Shapiro, Y.N.; O'Donnell, E.K. Oncologist perspective: Role of imaging in myeloma. *Skelet. Radiol.* **2022**, *51*, 123–133. [CrossRef]

36. Vicentini, J.R.T.; Bredella, M.A. Whole body imaging in musculoskeletal oncology: When, why, and how. *Skelet. Radiol.* **2023**, *52*, 281–295. [CrossRef]

37. Fain, J.N.; Madan, A.K.; Hiler, M.L.; Cheema, P.; Bahouth, S.W. Comparison of the release of adipokines by adipose tissue, adipose tissue matrix, and adipocytes from visceral and subcutaneous abdominal adipose tissues of obese humans. *Endocrinology* **2004**, *145*, 2273–2282. [CrossRef]

38. Himbert, C.; Delphan, M.; Scherer, D.; Bowers, L.W.; Hursting, S.; Ulrich, C.M. Signals from the Adipose Microenvironment and the Obesity-Cancer Link-A Systematic Review. *Cancer Prev. Res.* **2017**, *10*, 494–506. [CrossRef] [PubMed]

39. Arita, Y.; Kihara, S.; Ouchi, N.; Takahashi, M.; Maeda, K.; Miyagawa, J.; Hotta, K.; Shimomura, I.; Nakamura, T.; Miyaoka, K.; et al. Paradoxical decrease of an adipose-specific protein, adiponectin, in obesity. *Biochem. Biophys. Res. Commun.* **1999**, *257*, 79–83. [CrossRef]

40. Matsuzawa, Y. Establishment of a concept of visceral fat syndrome and discovery of adiponectin. *Proc. Jpn. Acad. Ser. B Phys. Biol. Sci.* **2010**, *86*, 131–141. [CrossRef]

41. Hofmann, J.N.; Liao, L.M.; Pollak, M.N.; Wang, Y.; Pfeiffer, R.M.; Baris, D.; Andreotti, G.; Lan, Q.; Landgren, O.; Rothman, N.; et al. A prospective study of circulating adipokine levels and risk of multiple myeloma. *Blood* **2012**, *120*, 4418–4420. [CrossRef]

42. Groß, J.P.; Nattenmüller, J.; Hemmer, S.; Tichy, D.; Krzykalla, J.; Goldschmidt, H.; Bertsch, U.; Delorme, S.; Kauczor, H.-U.; Hillengass, J.; et al. Body fat composition as predictive factor for treatment response in patients with newly diagnosed multiple myeloma—Subgroup analysis of the prospective GMMG MM5 trial. *Oncotarget* **2017**, *8*, 68460–68471. [CrossRef]

43. Panaroni, C.; Fulzele, K.; Mori, T.; Siu, K.T.; Onyewadume, C.; Maebius, A.; Raje, N. Multiple myeloma cells induce lipolysis in adipocytes and uptake fatty acids through fatty acid transporter proteins. *Blood* **2022**, *139*, 876–888. [CrossRef] [PubMed]

44. Marinac, C.R.; Birmann, B.M.; Lee, I.M.; Rosner, B.A.; Townsend, M.K.; Giovannucci, E.; Rebbeck, T.R.; Buring, J.E.; Colditz, G.A. Body mass index throughout adulthood, physical activity, and risk of multiple myeloma: A prospective analysis in three large cohorts. *Br. J. Cancer* **2018**, *118*, 1013–1019. [CrossRef] [PubMed]

45. Chang, S.H.; Luo, S.; Thomas, T.S.; O'Brian, K.K.; Colditz, G.A.; Carlsson, N.P.; Carson, K.R. Obesity and the Transformation of Monoclonal Gammopathy of Undetermined Significance to Multiple Myeloma: A Population-Based Cohort Study. *J. Natl. Cancer Inst.* **2017**, *109*, djw264. [CrossRef]

46. Landgren, O.; Rajkumar, S.V.; Pfeiffer, R.M.; Kyle, R.A.; Katzmann, J.A.; Dispenzieri, A.; Cai, Q.; Goldin, L.R.; Caporaso, N.E.; Fraumeni, J.F.; et al. Obesity is associated with an increased risk of monoclonal gammopathy of undetermined significance among black and white women. *Blood* **2010**, *116*, 1056–1059. [CrossRef] [PubMed]

47. Lee, D.J.; El-Khoury, H.; Tramontano, A.C.; Alberge, J.B.; Perry, J.; Davis, M.I.; Horowitz, E.; Redd, R.; Sakrikar, D.; Barnidge, D.; et al. Mass spectrometry-detected MGUS is associated with obesity and other novel modifiable risk factors in a high-risk population. *Blood Adv.* **2024**, *8*, 1737–1746. [CrossRef]

48. Boursi, B.; Weiss, B.M.; Haynes, K.; Mamtani, R.; Yang, Y.-X. Reappraisal of risk factors for monoclonal gammopathy of undetermined significance. *Am. J. Hematol.* **2016**, *91*, 581–584. [CrossRef]

49. Beason, T.S.; Chang, S.H.; Sanfilippo, K.M.; Luo, S.; Colditz, G.A.; Vij, R.; Tomasson, M.H.; Dipersio, J.F.; Stockerl-Goldstein, K.; Ganti, A.; et al. Influence of body mass index on survival in veterans with multiple myeloma. *Oncologist* **2013**, *18*, 1074–1079. [CrossRef]

50. Shah, U.A.; Whiting, K.; Devlin, S.; Ershler, R.; Kanapuru, B.; Lee, D.J.; Tahri, S.; Gwise, T.; Rustad, E.H.; Mailankody, S.; et al. Extreme body mass index and survival in newly diagnosed multiple myeloma patients. *Blood Cancer J.* **2023**, *13*, 13. [CrossRef]

51. Wennmann, M.; Goldschmidt, H.; Mosebach, J.; Hielscher, T.; Bäuerle, T.; Komljenovic, D.; McCarthy, P.L.; Merz, M.; Schlemmer, H.P.; Raab, M.S.; et al. Whole-body magnetic resonance imaging plus serological follow-up for early identification of progression in smouldering myeloma patients to prevent development of end-organ damage. *Br. J. Haematol.* **2022**, *199*, 65–75. [CrossRef] [PubMed]

52. Zamagni, E.; Nanni, C.; Gay, F.; Pezzi, A.; Patriarca, F.; Bello, M.; Rambaldi, I.; Tacchetti, P.; Hillengass, J.; Gamberi, B.; et al. 18F-FDG PET/CT focal, but not osteolytic, lesions predict the progression of smoldering myeloma to active disease. *Leukemia* **2016**, *30*, 417–422. [CrossRef] [PubMed]

53. Surov, A.; Thormann, M.; Wienke, A.; Ricke, J.; Seidensticker, M. Different cutoff values of the skeletal muscle mass and myosteatosis result in different clinical impact on overall survival in oncology. A subanalysis of a clinical trial. *J. Cancer Res. Clin. Oncol.* **2025**, *151*, 141. [CrossRef] [PubMed]